NJC

LETTER

DNA-controlled aggregation of virus like particles – mimicking a tetherin-like mechanism†

Daniela Serien,[ab] Christiane Grimm,[a] Jürgen Liebscher,[cd] Andreas Herrmann[a] and Anna Arbuzova*[a]

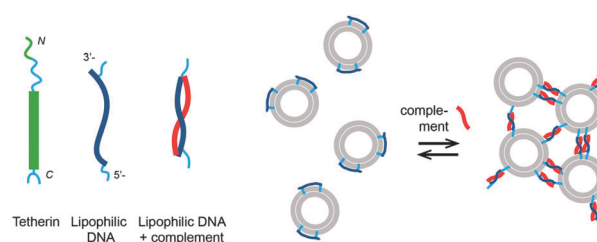**Mimicking cellular processes by functional comparable structures helps to understand their molecular mechanism. We report on an oligonucleotide modified with two α-tocopherol anchors mimicking tetherin, a cellular protein reducing spreading of viruses. The lipophilic DNA was incorporated into vesicles and virus like particles; their aggregation was induced by the complement addition.**

Nucleic acid is a versatile tool for bionanotechnology:[1–3] DNA-controlled assembly of structures is used to fabricate new materials and for development of drug delivery systems.[4–7] Recently, Chou *et al.* demonstrated that superstructures (built through DNA-controlled assembly of colloidal particles) showed improved accumulation in tumor.[5] The conjugation of a nucleic acid to a hydrophobic anchor allows attaching a molecular recognition unit to a lipid membrane.[8–10] Controlled assembly of vesicles, nanodiscs, and lipid layers, as well as hybridization-induced aggregation and fusion of lipid vesicles carrying lipophilic modifications were reported.[11–20]

Lipophilic nucleic acids have been used to mimic protein functions, *e.g.* channels[21] and SNARE proteins mediating fusion.[13,14,22] Here we suggest using a lipophilic oligonucleotide with two anchors to mimic tetherin/BST-2/CD317 function. Tetherin is an unusual cell protein with two membrane anchors – a transmembrane domain close to the N- and a glycophosphatidylinositol (GPI) anchor at the C-terminus; it was found on the cell surface and in endosomes. It is constitutively expressed in many human organs and cell lines,

e.g. in primary T lymphocytes and macrophages.[23,24] Tetherin was found to prevent the release of enveloped viruses from infected cells.[25] Viruses budding from the infected cells expressing tetherin stay first connected to the cell surface *via* tetherin, then are taken up and digested.[25,26] Tetherin-based chains of the viruses attached to the cell surface were observed by immunoelectron microscopy.[27] It was suggested that one of the membrane anchors of the tetherin stays in the cellular and the other is incorporated into the viral membrane.[25,26] This mechanism is reminiscent of the mechanism suggested for the aggregation of vesicles induced by lipophilic DNA (Scheme 1).[11,12] A lipophilic DNA with a hydrophobic anchor at each end binds first to the membrane of one liposome, as tetherin is incorporated into the plasma membrane *via* both N- and C-termini. Addition of the complementary DNA strand leads to the formation of a rigid DNA double helix (between the anchors). As the helix becomes oriented perpendicular to the lipid membrane driven by entropy, one of the anchors is pulled out of the membrane of the initial vesicle and might insert into another lipid vesicle.[11,12] Indeed, vesicles aggregated upon addition of lipophilic oligonucleotides of 17–27 nucleic bases (about 2–3 helical turns) modified with cholesteryl or palmitoyl anchors at both ends and the unmodified complementary strands.[11,12]

[a] *Humboldt-Universität zu Berlin, Institut für Biologie, Invalidenstr. 42, 10115 Berlin, Germany. E-mail: arbuzova@cms.hu-berlin.de*

[b] *The University of Tokyo, Institute of Industrial Science, 4-6-1 Komaba, Meguro-ku, Tokyo 153-8505, Japan*

[c] *Humboldt-Universität zu Berlin, Institut für Chemie, Brook-Taylor-Str. 2, 12489 Berlin, Germany*

[d] *National Institute of Research and Development for Isotopic and Molecular Technologies, Donath 65-103, Cluj-Napoca, Romania*

† Electronic supplementary information (ESI) available: Experimental details, structure of the α-tocopherol anchor, and results of the control measurements and details of the rate of the initial aggregation and virus like particles. See DOI: 10.1039/c4nj00724g

Scheme 1 A cartoon of tetherin, lipophilic DNA (LiNA), and DNA-induced aggregation of vesicles pre-incubated with LiNA. Membrane anchors and the transmembrane domain are shown in cyan. Hydrophilic regions of the protein and LiNA are shown in green and blue, respectively. Complementary oligonucleotide is shown in red.

Table 1 Sequences of the oligonucleotides used. TMR is tetramethylrhodamine and L is the α-tocopherol anchor

Name	Sequence
TL(dT)$_{18}$L(dT)$_5$	5′-TLT TTT TTT TTT TTT TTT TTL TTT TT-3′
(dA)$_{20}$	5′-AAA AAA AAA AAA AAA AAA AA-3′
(dT)$_{20}$	5′-TTT TTT TTT TTT TTT TTT TT-3′
3′Rh(dA)$_{20}$	5′-AAA AAA AAA AAA AAA AAA AA_TMR-3′
3′Rh(dT)$_{20}$	5′-TTT TTT TTT TTT TTT TTT TT_TMR-3′

Using α-tocopherol-modified thymine phosphoamidides, we have shown that the lipophilic anchor can be incorporated at any position of an oligonucleotide.[28,29] We observed that α-tocopherol-modified oligonucleotides incorporated spontaneously into preformed lipid vesicles within seconds, preferentially into the liquid-disordered phase, without significant perturbation of the lipid bilayer recommending such lipophilic oligonucleotides for functionalization of biological membranes.[30] Oligonucleotides modified with α-tocopherol at the terminal phosphate moiety were recently shown to incorporate spontaneously into cell membranes.[31] Here, we report investigations of a lipophilic oligonucleotide with two α-tocopherol anchors (L) separated by 18 bases and having additional 5 bases after the lipid anchor closer to the 3′end, TL(dT)$_{18}$L(dT)$_5$, termed LiNA. Sequences of the oligonucleotides are provided in Table 1.

The tocopherol anchors were attached to the nucleobase[29,32,33] rather than to the terminal phosphate moiety.[31,34] The structure of the anchor is shown in the ESI.† We characterized the LiNAs and their potential to function in a tetherin-like manner with model lipid vesicles and then verified it on HIV virus like particles (VLPs). Lacking regulatory proteins and genetic material, VLPs resemble morphologically native viruses but are noninfectious.[35]

We first show using fluorescence microscopy that the LiNA induced aggregation of model vesicles triggered by hybridization with a fluorescently labeled complementary strand, 3′Rh(dA)$_{20}$. Upon mixing of the LiNA, its complement (200 nM each), and POPC liposomes labeled with the fluorescent lipid analogue N-NBD-DPPE (400 μM total lipid), micrometer size aggregates were formed (Fig. 1A). For such high lipid concentrations, the resulting aggregates became visible even by the naked eye after a few minutes and precipitated if left undisturbed for several hours. Apparent co-localization of N-NBD and rhodamine signals revealed that in the presence of the LiNA 3′Rh(dA)$_{20}$
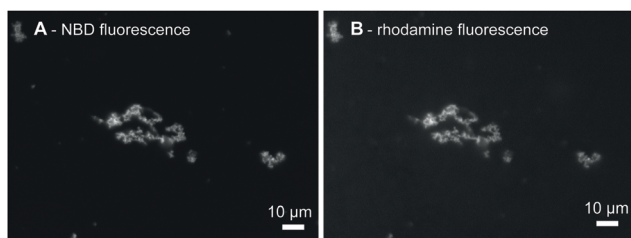
was accumulated within the aggregates (Fig. 1A and B). If either of the oligonucleotides was absent, no aggregation was observed: in the absence of LiNA rhodamine fluorescence was homogeneously distributed as shown in Fig. S1A, ESI.† Addition of a non-complementary strand neither induced any aggregation of the vesicles. The labeled non-complementary strands, 3′Rh(dT)$_{20}$, and the N-NBD-DPPE labeled vesicles were also distributed homogeneously in the presence and in the absence of the LiNA (Fig. S1B, ESI,† and not shown, respectively). Thus, hybridization of the LiNA and the complementary strand, 3′Rh(dA)$_{20}$, induced aggregation of lipid vesicles. We presume that in agreement with the mechanism suggested before[11,12,36] addition of 3′Rh(dA)$_{20}$ led to the formation of a rigid DNA helix between the anchors; as a consequence one of the α-tocopherol anchors was pulled out of the vesicle, where the LiNA was incorporated before, and could insert into another lipid vesicle.

We compared transition temperature of the LiNA with unlabeled complementary strand, (dA)$_{20}$, in the absence and the presence of POPC liposomes. In the absence of liposomes, dehybridization of LiNA/(dA)$_{20}$ was measured by following the increase in absorbance at 270 nm upon heating (Fig. 2A). The melting temperature, at which half of the hybrids de-hybridized, was about 38 °C. This melting temperature value indicates that according to the empirically based prediction algorithm 17 to 18 bases of TL(dT)$_{18}$L(dT)$_5$ in between the two lipid anchors are involved in DNA hybridization (e.g. OligoAnalyzer; Integrated DNA Technologies). For samples with vesicles, LiNA, and (dA)$_{20}$, a well-defined sharp transition, corresponding to the disassembly of the vesicle aggregates, was observed at 39.9 ± 0.2 °C by light scattering (Fig. 2B).

The width of the transition of 2.3 °C was much smaller than that of 10 °C observed in the absence of vesicles. Similarly, a smaller width for the disaggregation of DNA-linked 13 nm gold particles in comparison to that measured for unmodified DNA was reported previously and explained by the higher DNA density on the particles.[37] The sharp transition observed here can be explained by the effect of multiple connections between the vesicles (combinatorial entropic factors[38,39]) and a reduction of local salt concentration upon partial dehybridization.[37,40] In more detail, only at the contact sites of vesicles the distance
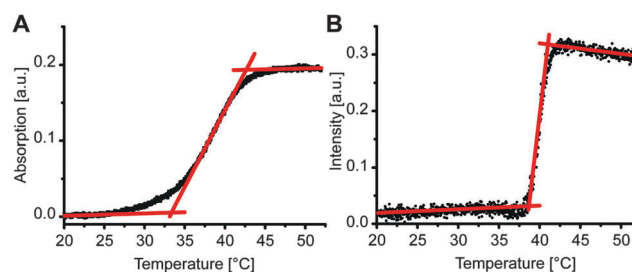

Fig. 1 Fluorescence microscopy images of the POPC/N-NBD-DPPE vesicle aggregates, 400 μM total lipid, induced by the hybridization of LiNA with 3′Rh(dA)$_{20}$, 200 nM each. (A) N-NBD, (B) rhodamine fluorescence images of the same area, respectively. Scale bars correspond to 10 μM.

Fig. 2 Determination of the transition temperatures of (A) melting of the LiNA/(dA)$_{20}$ hybrid, 480 nM, absorption at 270 nm; and (B) disassembly of the LiNA/(dA)$_{20}$ hybridization-induced vesicle aggregates, 400 μM POPC LUVs; light scattering at 600 nm. The width of the transition is ∼10 and 2.3 °C, respectively. Red lines are the linear fits of the initial, middle, and end regions used to determine transition temperatures and widths.

between vesicle membranes is small enough to enable the insertion of the two α-tocopherol anchors of a LiNA/(dA)$_{20}$ hybrid into the hydrophobic environment of the two opposing membranes. Outside the contact sites only one hydrophobic anchor of the stiff hybrid could insert into a membrane while the other would be exposed to the aqueous phase being energetically unfavorable. Hence, contact sites ensemble a trap enriching the hybrids locally. As a consequence, when raising temperature apparently cooperative dehybridization will occur caused by a change of DNA length and a reduction of local salt concentration upon partial dehybridization. The steep and sharp transition of vesicle disaggregation is in agreement with previous reports.[11,40,41]

Aggregation of the vesicles upon hybridization with an unlabeled complement was then measured by 90° light scattering (Fig. S2 and S3, ESI†) and UV absorption (Fig. 3A). We studied the dependence of the aggregation kinetics on the lipid concentration and observed that the rate of the aggregation increased with the increasing concentration (Fig. 3A). Therefore, not only the amount of DNA per vesicle,[17] but also the lipid concentration is crucial for the rate of the aggregation of the model vesicles. The initial rates were proportional to the ratio of the concentrations and lowest tested concentration c_0 by the power of $b = 2.2 \pm 0.2$ as shown in Fig. 3B. The second-order kinetics indicates that collision of two vesicles might be the rate limiting step for the initial aggregation (see ESI† for details).

Finally, based on the properties of the LiNA reported here, we suggest that a LiNA may act as a synthetic structure mimicking the function of tetherin which has membrane anchors at both N and C-termini and was shown to tether budding HIV viruses to the surface of the infected cells.[25–27] To this end, we investigated whether the LiNA hybridization can induce aggregation of HIV virus-like particles (VLPs).[35,42] VLPs are of 100–120 nm diameter and resemble native-like virions. Gag protein is required for the VLP formation; VLPs used here contained a fusion protein of Gag with YFP or mCherry.

We observed that addition of (dA)$_{20}$ to VLPs pre-incubated with the LiNA led to an increase in light scattering (Fig. 4A).

Fig. 4 Addition of LiNA and (dA)$_{20}$ to virus-like particles (VLPs) causes particle aggregation. (A) Light scattering at 310 nm upon addition of the LiNA at 260 s and (dA)$_{20}$ at 510 s (black curve) or upon addition of (dA)$_{20}$ at 500 s (red curve) to 15 μL VLPs in 1 mL buffer, 37 °C; Fluorescence microscopy images of VLPs (5 μL VLPs in 50 μL buffer) pre-incubated with the LiNA, 200 nM for 30 min: before (B) and 10 min after addition of (dA)$_{20}$, 200 nM (C). Scale bars correspond to 10 μM.

The scattering experiments required 1 mL sample volume for stirring, therefore, only a very low concentration of VLPs could be used. The increase in scattering is rather low, nevertheless, it is comparable with the increase in scattering for the similarly low concentration of lipid vesicles (see Fig. 3A, 55 μM). Using higher VLP concentrations (in a smaller volume), aggregates were also detected using a microscope 10 min after addition of the complement to VLPs pre-incubated with LiNA for 30 min (Fig. 4B and C). The results show that tocopherol anchors could easily insert into the lipid envelope of the VLPs and cause aggregation due to DNA-hybridization and accompanied exposure of hydrophobic anchors as described above for model vesicles. Indeed this VLP aggregation is reminiscent of the chain-like aggregation of HIV viruses attached on the cell surface observed by electron microscopy.[27]

While the density of spike proteins in the HIV envelope is rather low, other enveloped viruses have a very high density of spike proteins, e.g. hemagglutinin, the major surface protein of the Influenza viruses, covers more than 80% of the surface and is at least 13 nm high.[43,44] To trigger aggregation of such viruses it may require longer DNA-strands as used here. This conclusion is supported by a recent report of Selden et al.[45] who showed that a long linker of at least 60 nucleic bases was necessary for cell–cell attachment. Recently, cholesterol-modified PEG presented on a glass surface via biotin/avidin was used to immobilize lipid vesicles, viruses, bacteria, and yeast cells.[46] Hence, also for a controlled and more efficient virus aggregation, a longer lipophilic nucleic acid with a longer sequence or a linker might be required.

Lipophilic nucleic acids modified with two palmitoyl chains or cholesterol partitioning into raft domains specifically were recently reported by us and others.[10,47–49] Application of different lipophilic anchors allows sequestration of the LiNAs in domains and a remote control of the functional moieties by temperature[48] or enzymatic cleavage.[49] As tetherin was found to localize in rafts,[50] a similarly built LiNA with a longer sequence and two anchors partitioning into raft-like domains, e.g. cholesterol or palmitoyl anchors, might even better mimic tetherin.

Taken together, we have shown here that aggregation of HIV virus-like particles, likewise to the aggregation of lipid vesicles, can be achieved using the lipophilic nucleic acid with two lipophilic anchors each close to one end of the sequence.
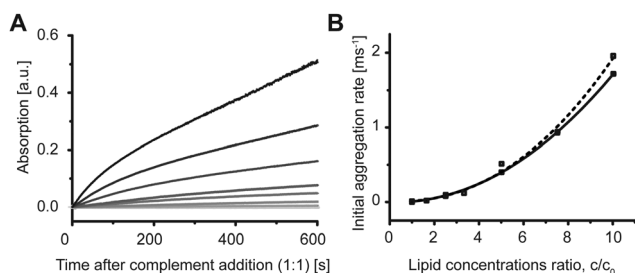

Fig. 3 POPC DNA-hybridization induced vesicle aggregation depends on lipid/vesicle concentration. (A) POPC vesicles were pre-incubated with 200 nM LiNA. Addition of (dA)$_{20}$ at time 0 s induced aggregation and, therefore, increase in turbidity of the sample measured at 400 nm. The rate and the intensity of the signal increased with increasing lipid concentration as shown for 0, 55, 90, 150, 170, 270, 450, and 540 μM lipid. (B) Second order dependence of the initial rate on the ratio of the lipid concentrations c/c_0, where $c_0 = 55$ μM. Squares are data points from two independent experiments. Lines are the fitting curves $f(x) = ax^b$ with $b = 2.2 \pm 0.2$.
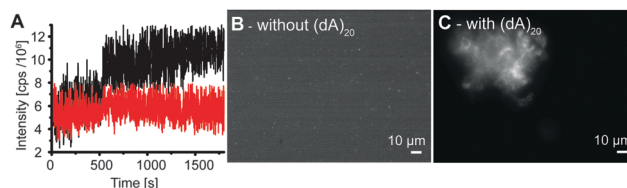
Experimental

The sequence of the addition of the oligonucleotides was not essential for the aggregation process (Fig. S2, ESI†); however, the initial aggregation rates were slightly higher when vesicles were pre-incubated with the LiNA. HIV virus like particles labeled with mCherry or YFP were isolated as described elsewhere[42] and were a kind gift of Andrea Gramatica. For details of VLPs see ESI.† Total protein concentration of the VLP stocks was about 0.8 mM.

Notes and references

1 P. X. Guo, *Nat. Nanotechnol.*, 2010, **5**, 833–842.
2 Y. Krishnan and F. C. Simmel, *Angew. Chem., Int. Ed.*, 2011, **50**, 3124–3156.
3 N. C. Seeman, *Nature*, 2003, **421**, 427–431.
4 Y. Wu, K. Sefah, H. Liu, R. Wang and W. Tan, *Proc. Natl. Acad. Sci. U. S. A.*, 2010, **107**, 5–10.
5 L. Y. Chou, K. Zagorovsky and W. C. Chan, *Nat. Nanotechnol.*, 2014, **9**, 148–155.
6 O. Pokholenko, A. Gissot, B. Vialet, K. Bathany, A. Thiéry and P. Barthélémy, *J. Mater. Chem. B*, 2013, **1**, 5329–5334.
7 A. Aimé, N. Beztsinna, A. Patwa, A. Pokolenko, I. Bestel and P. Barthélémy, *Bioconjugate Chem.*, 2013, **24**, 1345–1355.
8 H. Rosemeyer, *Chem. Biodiversity*, 2005, **2**, 977–1063.
9 D. Berti, C. Montis and P. Baglioni, *Soft Matter*, 2011, **7**, 7150–7158.
10 M. Schade, D. Berti, D. Huster, A. Herrmann and A. Arbuzova, *Adv. Colloid Interface Sci.*, 2014, **208**, 235–251.
11 U. Jakobsen, A. C. Simonsen and S. Vogel, *J. Am. Chem. Soc.*, 2008, **130**, 10462–10463.
12 G. Zhang, F. Farooqui, O. Kinstler and R. L. Letsinger, *Tetrahedron Lett.*, 1996, **37**, 6243–6246.
13 G. Stengel, R. Zahn and F. Höök, *J. Am. Chem. Soc.*, 2007, **129**, 9584–9585.
14 G. Stengel, L. Simonsson, R. A. Campbell and F. Höök, *J. Phys. Chem. B*, 2008, **112**, 8264–8274.
15 T. Maruyama, H. Yamamura, M. Hiraki, Y. Kemori, H. Takata and M. Goto, *Colloids Surf., B*, 2008, **66**, 119–124.
16 A. Bunge, M. Loew, P. Pescador, A. Arbuzova, N. Brodersen, J. Kang, L. Dähne, J. Liebscher, A. Herrmann, G. Stengel and D. Huster, *J. Phys. Chem. B*, 2009, **113**, 16425–16434.
17 P. A. Beales and T. K. Vanderlick, *J. Phys. Chem. A*, 2007, **111**, 12372–12380.
18 P. A. Beales, C. L. Bergstrom, N. Geerts, J. T. Groves and T. K. Vanderlick, *Langmuir*, 2011, **27**, 6107–6115.
19 P. A. Beales and T. K. Vanderlick, *Adv. Colloid Interface Sci.*, 2014, **207**, 290–305.
20 B. van Lengerich, R. J. Rawle, P. M. Bendix and S. G. Boxer, *Biophys. J.*, 2013, **105**, 409–419.
21 J. R. Burns, K. Göpfrich, J. W. Wood, V. V. Thacker, E. Stulz, U. F. Keyser and S. Howorka, *Angew. Chem., Int. Ed.*, 2013, 1–5.
22 Y.-H. M. Chan, B. van Lengerich and S. G. Boxer, *Biointerphases*, 2008, **3**, FA17.
23 E. Erikson, T. Adam, S. Schmidt, J. Lehmann-Koch, B. Over, C. Goffinet, C. Harter, I. Bekeredjian-Ding, S. Sertel, F. Lasitschka and O. T. Keppler, *Proc. Natl. Acad. Sci. U. S. A.*, 2011, **108**, 13688–13693.
24 S. J. D. Neil, T. Zang and P. D. Bieniasz, *Nature*, 2008, **451**, 425–430.
25 J. Hammonds and P. Spearman, *Cell*, 2009, **139**, 456–457.
26 S. Venkatesh and P. D. Bieniasz, *PLoS Pathog.*, 2013, **9**, e1003483.
27 J. Hammonds, J.-J. Wang, H. Yi and P. Spearman, *PLoS Pathog.*, 2010, **6**, e1000749.
28 A. Kurz, A. Bunge, A.-K. Windeck, M. Rost, W. Flasche, A. Arbuzova, D. Strohbach, S. Müller, J. Liebscher, D. Huster and A. Herrmann, *Angew. Chem., Int. Ed.*, 2006, **45**, 4440–4444.
29 W. Flasche, C. Cismas, A. Herrmann and J. Liebscher, *Synthesis*, 2004, 2335–2341.
30 A. Bunge, A. Kurz, A.-K. Windeck, T. Korte, W. Flasche, J. Liebscher, A. Herrmann and D. Huster, *Langmuir*, 2007, **23**, 4455–4464.
31 T. Tokunaga, S. Namiki, K. Yamada, T. Imaishi, H. Nonaka, K. Hirose and S. Sando, *J. Am. Chem. Soc.*, 2012, **134**, 9561–9564.
32 N. Brodersen, J. Li, O. Kaczmarek, A. Bunge, L. Löser, D. Huster, A. Herrmann and J. Liebscher, *Eur. J. Org. Chem.*, 2007, 6060–6069.
33 O. Kaczmarek, N. Brodersen, A. Bunge, L. Löser, D. Huster, A. Herrmann, A. Arbuzova and J. Liebscher, *Eur. J. Org. Chem.*, 2008, 1917–1928.
34 K. Nishina, T. Unno, Y. Uno, T. Kubodera, T. Kanouchi, H. Mizusawa and T. Yokota, *Mol. Ther.*, 2008, **16**, 734–740.
35 L. Deml, C. Speth, M. P. Dierich, H. Wolf and R. Wagner, *Mol. Immunol.*, 2005, **42**, 259–277.
36 U. Jakobsen and S. Vogel, *Bioconjugate Chem.*, 2013, **24**, 1485–1495.
37 R. Jin, G. Wu, Z. Li, C. A. Mirkin and G. C. Schatz, *J. Am. Chem. Soc.*, 2003, **125**, 1643–1654.
38 S. Angioletti-Uberti, P. Varilly, B. M. Mognetti, A. V. Tkachenko and D. Frenkel, *J. Chem. Phys.*, 2013, **138**, 021102.
39 P. Varilly, S. Angioletti-Uberti, B. M. Mognetti and D. Frenkel, *J. Chem. Phys.*, 2012, **137**, 094108.
40 P. A. Beales and T. K. Vanderlick, *Biophys. J.*, 2009, **96**, 1554–1565.
41 N. Dave and J. Liu, *ACS Nano*, 2011, **5**, 1304–1312.
42 M. Perlman and M. D. Resh, *Traffic*, 2006, **7**, 731–745.
43 C. Böttcher, K. Ludwig, A. Herrmann, M. van Heel and H. Stark, *FEBS Lett.*, 1999, **463**, 255–259.
44 A. K. Harris, J. R. Meyerson, Y. Matsuoka, O. Kuybeda, A. Moran, D. Bliss, S. R. Das, J. W. Yewdell, G. Sapiro,

K. Subbarao and S. Subramaniam, *Proc. Natl. Acad. Sci. U. S. A.*, 2013, **110**, 4592–4597.

45 N. S. Selden, M. E. Todhunter, N. Y. Jee, J. S. Liu, K. E. Broaders and Z. J. Gartner, *J. Am. Chem. Soc.*, 2012, **134**, 765–768.

46 P. Kuhn, K. Eyer, T. Robinson, F. I. Schmidt, J. Mercer and P. S. Dittrich, *Integr. Biol.*, 2012, **4**, 1550–1555.

47 P. A. Beales, J. Nam and T. K. Vanderlick, *Soft Matter*, 2011, **7**, 1747–1755.

48 M. Loew, R. Springer, S. Scolari, F. Altenbrunn, O. Seitz, J. Liebscher, D. Huster, A. Herrmann and A. Arbuzova, *J. Am. Chem. Soc.*, 2010, **132**, 16066–16072.

49 M. Schade, A. Knoll, A. Vogel, O. Seitz, J. Liebscher, D. Huster, A. Herrmann and A. Arbuzova, *J. Am. Chem. Soc.*, 2012, **134**, 20490–20497.

50 P. G. Billcliff, R. Rollason, I. Prior, D. M. Owen, K. Gaus and G. Banting, *J. Cell Sci.*, 2013, **126**, 1553–1564.